P2.22

AEROSOL OPTICAL DEPTH OVER LAND FROM THE AVHRR PATHFINDER ATMOSPHERE DATA SET

Kenneth R. Knapp*
CIRA –NOAA/NESDIS/ORA

1. INTRODUCTION

With the reprocessing of AVHRR data back to 1981 by the AVHRR Pathfinder Atmosphere (PATMOS) project at NOAA/NESDIS (Jacobowitz, 1999), cloud-free radiance statistics exist for each day on a global 110 km grid for all five channels of AVHRR. Ocean grid cell data have been processed with the NOAA operational aerosol retrieval algorithm to create the most extensive record of aerosol optical depth (τ) ever compiled. However, as theoretical climate model studies indicate, the most significant concentrations and radiative effects of aerosols occur over land. To assist these climate studies, as well as the Global Aerosol Climatology Project, we are developing a τ retrieval algorithm over land comparable to the one over oceans when and where an aerosol signal is present in the 0.63μm reflectance channel of AVHRR.

The first step of this research was to determine an aerosol signal in the PATMOS data, where a signal was found, but is strongly dependent on the surface bidirectional reflectance distribution function (BRDF). The research presented herein is the preliminary results of retrieving aerosol optical depth from top-of-the-atmosphere (TOA) AVHRR PATMOS reflectances.

2. DATA

Two data sources are used in this study: the PATMOS data set provides cloud-free TOA reflectance observations and the Aerosol Robotic Network (AERONET) data provide ground-truth aerosol optical depths.

2.1 PATMOS Data

The Advanced Very High Resolution Radiometer (AVHRR) has flown nearly continuously on numerous NOAA satellites since 1981. This vast amount of data is condensed into a useable format in the PATMOS data set (Jacobowitz et al., 2001; Stowe et al., 2001). The volume of the Global Area Coverage (GAC) AVHRR data has been significantly reduced from terabytes to gigabytes by statistically decreasing the spatial resolution. The GAC data are binned into 110×110 km^2 quasi-equal area grid cells where statistics are calculated for each AVHRR channel for each grid cell.

The PATMOS daily-radiance data set (PATMOS-1) includes 71 parameters for each grid cell. 54 parameters are direct variables of AVHRR measurements. Four statistical categories are used for each channel: All pixels, clear sky, aerosol burden and cloudy. Statistics for each category (generally, the mean and standard deviation) are recorded for each channel. The parameter used in this study is the channel 1 (0.63μm) reflectance (R_{sat}) deemed cloud-free by the CLAVR-1 algorithm (Stowe et al., 1999).

For this study, the PATMOS-1 data from 1993 through 1999 are used to compare with AERONET observations of τ.

2.2 AERONET Data

The AERONET provides the ground truth validation for this research. AERONET is a federation of sun-sky radiometers independently owned with centrally archived data, which can measure aerosol optical depth to an accuracy of ±0.02 (Holben et al., 1998). Data used in this study utilizes only those sites where the data have been cloud filtered as well as post-calibrated (i.e., level 2 data).

3. AEROSOL RETRIEVAL METHOD

The retrieval of aerosol information from PATMOS data over land is a three-step process. First, reflectances for numerous conditions are calculated from a radiative transfer model and stored in look-up tables (LUT). These tables are then used to retrieve the surface BRDF from the PATMOS data. The surface BRDF data are then used to retrieve τ from the PATMOS data using LUT for that BRDF. This method is developed and further test by Knapp and Stowe (2001).

3.1 Step 1: Look-Up Table Calculation

The DISORT radiative transfer model version 2 (Tsay et al. 2000) is used to produce theoretical TOA reflectances. TOA reflectances (R_{LUT}) were simulated at 13 solar zenith angles, θ_1: 10°-70°, 15 satellite zenith angles, θ_2: 0°-70° and 19 azimuth

* Corresponding author address: Kenneth Knapp; CIRA-NOAA/NESDIS/ORA; Room 711c; 5200 Auth Rd.; Camp Springs, MD, 20746-4304; email: Ken.Knapp@noaa.gov

angles, ϕ_1-ϕ_2: 0°-180°. Atmospheric effects were held constant during the calculations, with ozone absorption and Rayleigh scattering characteristic of a tropical atmosphere.

Privette et al. (1997) compare different BRDF models and conclude that the model described by Rahman et al. (1993) describes a multitude of surfaces with higher accuracy than other models. Therefore, it was used in this research to model the surface; it uses three terms to describe the surface: the magnitude of the surface reflectance, ρ; the Henyey-Greenstein function parameter, Θ; and the level of anisotropy, k. For each viewing geometry in the LUT, calculations were performed at 1100 BRDF combinations, with ρ: 0.001 to 0.09, Θ: -1 to 1, and k: 0.0 to 1. Each BRDF was used in a DISORT run to calculate the R_{sat} due to the surface BRDF and Rayleigh scattering for each of the 3705 possible geometries.

Lastly, aerosol scattering and absorption are included in these calculations via the continental aerosol described by Kaufman et al (1997). One look-up table is computed with $\tau = 0.05$. This is the assumed to be the minimum τ observed during the composite time period. LUTs area also calculated at other τ values, the interpolation between which allows the τ retrieval.

3.2 Step 2: Surface BRDF Retrieval

The surface BRDF is estimated by compositing PATMOS reflectances. The satellite repeat cycle of the NOAA series of satellites is nine days. Thus, over the course of 24 days it is possible to composite 3 observations from each look angle (given plenty of cloud-free observations). However at some sites, cloudy skies limit the number of observations, so the time period is allowed to vary from 24 to 48 days. Circles in figure 1 show an example of 24 days of cloud-free channel 1 reflectances from the Patmos-1 data. It is clear that a significant trend as a function of view zenith angle is present and that there is noise in this trend. Assuming that the presence of aerosol increases the reflectance (i.e., that the aerosol absorption is low), then the darkest of these points in the composite is likely to have the lowest τ.

The LUT with $\tau = 0.05$ is used to determine the surface BRDF. First, the LUT is interpolated for the viewing geometry of each of the points. This narrows the possible solutions to the 3705 combinations of BRDF parameters. A cost function is then used to retrieve the best-fit BRDF parameters.

An example BRDF retrieval is also shown in figure 1. The circles represent PATMOS observations over Cuiaba, Brazil. The squares represent the TOA reflectances given the retrieved BRDF. In general, the squares compare well with the darkest observed reflectances.

This BRDF retrieval method is not limited to AERONET locations since the retrieval of BRDF parameters uses only the PATMOS data. It can be used over the entire world regardless of ground-truth location. However, the accuracy of the aerosol retrieval will depend on location so current retrievals are limited to AERONET sites.

3.3 Step 3: Aerosol Optical Depth Retrieval

Once the BRDF parameters have been determined, the τ retrieval is performed. The LUTs for each τare interpolated to the corresponding BRDF parameters and viewing geometry. Finally, τ is retrieved by matching the R_{sat} within the LUT to the corresponding τ. Before discussing the retrieval results, the uncertainty in these comparisons should be considered.

4. UNCERTAINTIES

Perhaps the most significant is the sampling of cloud-free pixels in the PATMOS grid cell. The surface viewed each day varies with the spatial distribution of cloud. So for spatially inhomogeneous areas, the day-to-day variation in the observed surface can be large.

Another source of noise is the difference of the AERONET instrument field-of-view of the Sun and the $110 \times 110 km^2$ spatial resolution of the PATMOS data. Thus, spatial variations in τ will increase noise in the comparison.

Other uncertainties result from departure of the actual conditions from those assumed in the LUT, which include variations in:

- aerosol optical properties (spatially and temporally)
- column ozone amount
- Rayleigh scattering optical depth
- cloud contamination in the PATMOS cloud-free reflectances
- the lowest observed τ (because 0.05 is assumed)
- the discrepancy between the modeled BRDF and the actual BRDF

5. RESULTS

Retrievals are applied to PATMOS land grid cells nearest to 122 of the AERONET sites around the world between 1993 and 1999 (which covers the seven years of level-2 AERONET data).

The validation of the Cuiaba retrieval is shown in figure 2. Currently, the retrieval validation is filtered for:

- Standard deviation of the PATMOS cloud-free reflectances > 0.05: too large of a spatial variance
- View Zenith Angle < 0°: Staying away from the backscatter peak reflectance
- Fraction of cloud free pixels in the grid cell: Requires the cloud free pixels to be greater than one-third the number of all pixels.

These restraints on the validation with ground truth decrease the noise when verifying with the AERONET point measurement. For Cuiaba, the correlation, r, is 0.88 with a root-mean-square difference of 0.15. There is a negative bias (i.e., slope of 0.78) likely due to the larger absorption of the typical biomass-burning aerosol than the continental aerosol of the LUT.

Grouping all the AERONET sites in South America provides more insight to the retrieval performance (figure 3). A similar low bias (with a slope of 0.63) and correlation (r = 0.87) is found. However, the retrieval shows significant errors during August and September (the burning season) when the assumed background τ (0.05) is likely wrong. Error analysis, together with independent observations and models of the surface and atmosphere, will allow us to analyze error sources and increase the accuracy of the retrieval method.

Further grouping of results into ten regions provides analysis for sites over the globe. These results are preliminary; yet still suggest where this approach is appropriate. Statistics for the ten regions are presented in Table 1. It is clear that the best results are in South America where the surface reflectance has small temporal and spatial variations and the aerosol is relatively constant (aerosol here are primarily from biomass burning). Other regions with high correlations include southern Africa, Central Canada and parts of the U.S.

5. CONCLUSIONS

The surface BRDF is retrieved from PATMOS channel 1 cloud-free reflectance data and used to retrieve the aerosol optical depth. Comparisons of retrieved τ to ground-truth show positive correlation in all defined regions of the globe. However, the correlations are weak in some areas, likely due to:

- Desert areas have a brighter reflectance than used in the LUT BRDF calculations
- TOA reflectance is less sensitive to aerosols over brighter areas.
- Other uncertainty sources as described in section 4.

Further research will include:

- More error analysis to determine error sources.
- Inclusion of multiple aerosol types in the LUTs to remove regional biases.
- Inclusion of other ground-truth data sets, e.g., the Multi-Filter Rotating Shadowband Radiometer (MFRSR) AOD dataset
- Inclusion of surface information from channel 2 (0.83μm)

The addition of this information should increase the accuracy (and thus, value) of the retrieval of AOD from the PATMOS data set.

The current results are encouraging. The retrieval of aerosol optical depth over land has been very limited and these results suggest the possibility of quantifying spatial and temporal variation of aerosol optical depth over some land areas within the 20-year record of the PATMOS data set.

ACKNOWLEDGMENTS

This work is supported by the NASA/Global Aerosol Climatology Project (GACP, Michael Mishchenko, Principal Scientist). We acknowledge Brent Holben of NASA and the Principle Investigators of each AERONET site for the use of their data, which is available at http://aeronet.gsfc.nasa.gov:8080/ and the personnel of NOAA Satellite Active Archive where the PATMOS data can be acquired (http://www.saa.noaa.gov/).

REFERENCES

Holben, B. N. et al., 1998: AERONET – A Federated Instrument Network and Data Archive for Aerosol Characterization, Remote Sens. Environ., 66, 1-16.

Jacobowitz, H., L. Stowe, G. Ohring, K. Knapp and N. Nalli, 2001: The Advanced Very High Resolution Radiometer Pathfinder Atmosphere Data Set, submitted to *Bull. Amer. Meteor. Soc.*

Kaufman, Y. J., D. Tanré, L. A. Remer, E. F. Vermote, A. Chu and B. N. Holben,1997: Operational remote sensing of tropospheric aerosol over land from EOS moderate resolution imaging spectro-radiometer, J. Geophys. Res., 102, 17051-17068.

Knapp, K. R. and L. L. Stowe, 2001: Evaluating the potential for retrieving aerosol optical depth over land from AVHRR Pathfinder Atmosphere data, accepted to *J. Atmos. Sci.*

Privette, J. L., T. F. Eck and D. W. Deering, 1997: Estimating spectral albedo and nadir reflectance through inversion of simple BRDF models with AVHRR/MODIS-like data, J. Geophys. Res., 102, 29529-29542.

Rahman, H., B. Pinty and M. M. Verstraete, 1993: Coupled Surface-Atmosphere Reflectance Model 2. Semiempirical Surface Model Usable with NOAA Advanced Very High Resolution Radiometer Data, J. Geophys. Res., 98, 20791-20801.

Stowe, L. L., P. A. Davis and E. P. McClain, 1999: Scientific Basis and Initial Evaluation of the CLAVR-1 Global Clear/Cloud Classification Algorithm for the Advanced Very High Resolution Radiometer, J. Atm. Oceanic Tech., 16, 656-681.

Stowe, L. L., H. Jacobowitz, G. Ohring, K. Knapp and N. Nalli, 2001: The Advanced Very High Resolution Radiometer Pathfinder Atmosphere Data Set, submitted to *J. Climate*.

Tsay, Si-C., K. Stamnes, W. Wiscombe, and I. Laszlo, 2000: General Purpose Fortran Program for Discrete-Ordinate-Method Radiative Transfer in Scattering and Emitting Layered Media: An Update of DISORT, presented at the International Radiation Symposium 2000, in St. Petersburg, Russia.

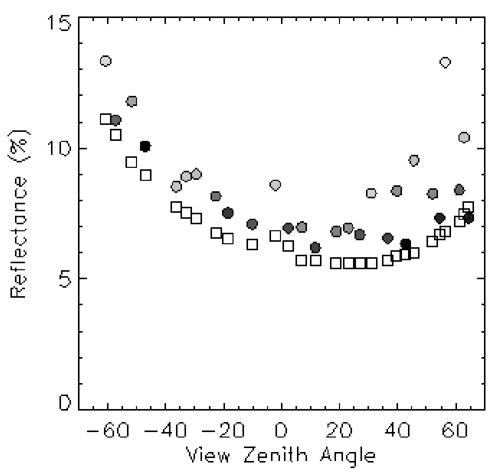

Figure 1 – Example fit of PATMOS cloud-free observations (circles) to a BRDF (squares) at Cuiaba, Brazil. The retrieved parameters BRDF are ρ = 0.03, k = 0.1, and Θ = 0.1. Negative viewing angle corresponds to viewing away from the Sun.

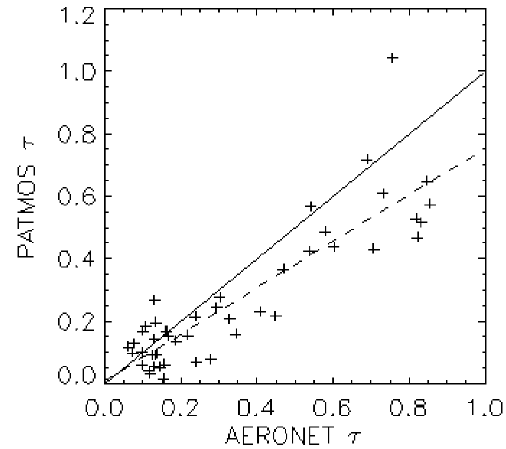

Figure 2 – Validation of filtered PATMOS AOD with AERONET AOD at Cuiaba. The linear regression best fit (dashed line) is: y=0.78x + 0.01 with r = 0.88 (for 47 points)

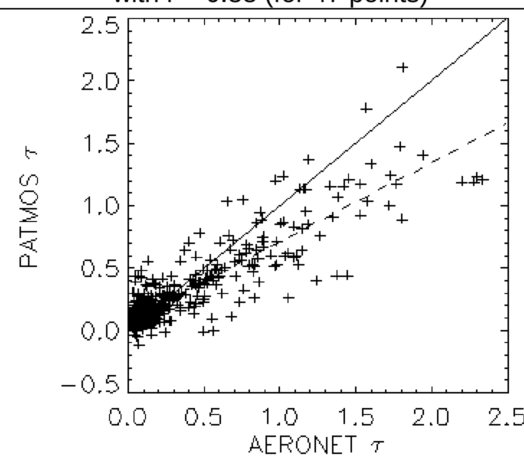

Figure 3 – Validation of filtered PATMOS AOD with AERONET AOD for South America. The linear regression best fit (dashed line) is: y=0.63x + 0.08 with r = 0.87 (for 396 points)

Table 1 – Statistics of the filtered validation of AOD estimation for different regions of the world.

Region	n	r	Slope	Offset
South America	**396**	**0.87**	**0.63**	**0.08**
Northwestern U.S.	101	0.33	0.81	0.11
Southwestern U.S.	293	0.16	0.75	0.27
Midwestern U.S.	**216**	**0.55**	**0.75**	**0.11**
Eastern U.S.	431	0.49	0.47	0.14
Central Canada	**240**	**0.87**	**0.75**	**0.06**
Europe	208	0.49	0.53	0.13
Western Africa	374	0.29	0.71	0.44
Southern Africa	**249**	**0.66**	**0.55**	**0.09**
Other*	468	0.15	0.80	0.60

* All other sites outside the defined regions